NUCLEAR THEORY, Vol. 40 (2023)
eds. M. Gaidarov, N. Minkov, Heron Press, Sofia

The Multiple Personalities of Low-Density Neutron Matter

F. Sammarruca

Department of Physics, University of Idaho, Moscow, Idaho 83844-0903, USA

Abstract. We will provide a brief summary of the status regarding the density dependence of the symmetry energy and related issues of contemporary interest. We will then move to the recent measurement of the neutron skin in ^{48}Ca and discuss it in the context of existing measurements and predictions. We will close with our current work on low-density neutron matter and the unitary limit. The overarching theme is the importance of constraints from low-energy few-nucleon physics for neutron matter and the symmetry energy.

1 Introduction

The physics of neutron matter (NM) spans a broad range of densities. At low density, it approaches universal behavior as a consequence of the large neutron-neutron scattering length in the spin-singlet channel. Around normal nuclear density, it is an appropriate laboratory to study neutron-rich nuclei, and, at even higher densities, it constrains the physics of neutron stars. Although an idealized system, neutron matter provides unique opportunities to test nuclear forces, because all low-energy constants appearing in the three-neutron forces are predicted at the two-neutron level.

Isospin-asymmetric nuclear matter is characterized by the degree of neutron excess, all the way to pure neutron matter. Of paramount importance for the description of isospin-asymmetric nuclear system is the symmetry energy. In the so-called parabolic approximation for the equation of state (EoS) of isospin-symmetric nuclear matter,

$$e(\rho,\alpha) \approx e_0(\rho) + e_{\rm sym}(\rho)\,\alpha^2\ , \tag{1}$$

where $\alpha = (\rho_n - \rho_p)/\rho$, the symmetry energy becomes

$$e_{\rm sym}(\rho) = e_n(\rho) - e_0(\rho)\ , \tag{2}$$

where $e_n(\rho)$ is the energy per neutron in pure NM, and $e_0(\rho)$ is the energy per nucleon in symmetric nuclear matter (SNM). Expanding the symmetry energy about the saturation point, we obtain

$$e_{\rm sym}(\rho)\ \approx\ e_{\rm sym}(\rho_0) + L\,\frac{\rho-\rho_0}{3\rho_0} + \frac{K_{\rm sym}}{2}\frac{(\rho-\rho_0)^2}{(3\rho_0)^2}\ , \tag{3}$$

which helps identifying several useful parameters. L is known as the slope parameter, as it is a measure of the slope of the symmetry energy at saturation:

$$L = 3\rho_0 \Big(\frac{\partial e_{\rm sym}(\rho)}{\partial \rho} \Big)_{\rho_0} \ . \tag{4}$$

Furthermore, it is clear from Eqs. (2) and (4), recalling that the SNM EoS has vanishing derivative at that point, that L measures the degree of "stiffness" of the NM EoS at saturation density. The symmetry energy slope, essentially a pressure gradient acting on excess neutrons in the neutron-enriched core, determines the formation and size of the neutron skin.

Since many years several groups have sought constraints on the density dependence of the symmetry energy. Intense experimental effort has been and continues to be devoted to this question using various measurements, which are typically analyzed with the help of correlations obtained through different parametrizations of phenomenological models. Here, we will emphasize the importance of the *ab initio* approach towards robust predictions of NM and the symmetry energy.

We will also discuss our on-going work on low-density NM, with emphasis on the unitary limit as a constraint for the symmetry energy.

2 Brief Review of Theoretical Tools

The interactions we use are derived from chiral effective field theory (EFT) [1], which provides a path to a consistent development of nuclear forces. Symmetries relevant to low-energy QCD are incorporated in the theory, in particular chiral symmetry. Thus, although the degrees of freedom are pions and nucleons instead of quarks and gluons, there exists a solid connection with the fundamental theory of strong interactions through its symmetries and the mechanism of their breaking. Chiral EFT employs a power counting scheme in which the progression of two- and many-nucleon forces is constructed following a well-defined hierarchy. This allows for the inclusion of all three-nucleon forces (3NFs) which appear at a given order, thus eliminating the inconsistencies which are unavoidable when adopting meson-theoretic or phenomenological forces. Finally, it provides a clear method for controlling the truncation error at each order. Detailed information on our calculations, including the values of the LECs, can be found in Refs. [2, 3].

The EoS for neutron matter is obtained at the leading-order in the hole-line expansion—namely, via a non-perturbative summation of the particle–particle ladders. The single-neutron potentials are computed self-consistently with the G-matrix, employing a continuous spectrum.

3 Neutron Matter: Impact of the Isovector Component of the Free-Space Nucleon-Nucleon Force

In the impressive analysis in Ref. [4], 10^9 nuclear force parametrizations consistent with chiral EFT are examined. Employing state-of-the-art statistical methods and computational technology, the authors are able to make quantitative predictions for bulk properties and skin thickness of ^{208}Pb. In the process, they find a strong correlation between L and the $^1S_0$ phase shift at laboratory energies around 50 MeV.

We performed a calculation which serves as a simple and transparent test of the impact of the isovector part of the free-space NN force in neutron matter. We consider 2NFs only.

For the purpose of this test, we constructed a version of the N^{3}LO(450) potential where the fit of isospin-1 partial waves is deteriorated as compared to the original potential, see Figure 1. This is accomplished by adjusting two LECs in $^1S_0$ channel and one LEC for each of the P-waves (all changes are on average between 2 and 10%), while keeping the scattering length at its correct value. Although not dramatic, the impact on the phase shifts is considerable, especially

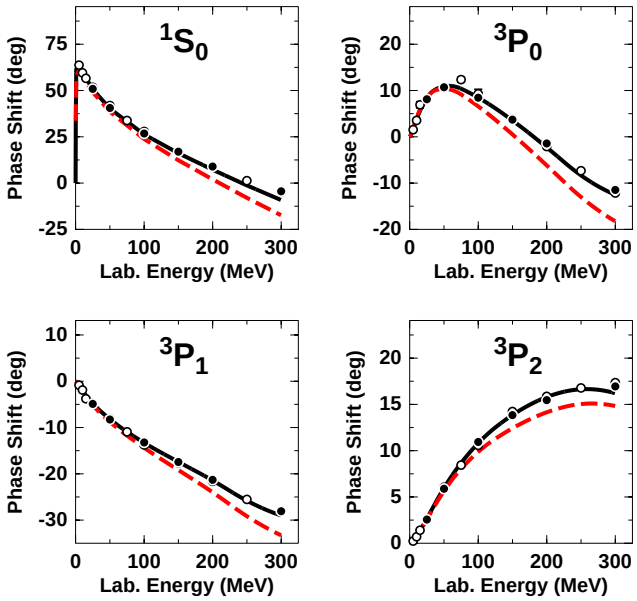

Figure 1. Phase shifts for selected isospin-1 partial waves as a function of the laboratory energy. Solid black: original N^{3}LO(450) potential; Red dash: modified version as explained in the text..

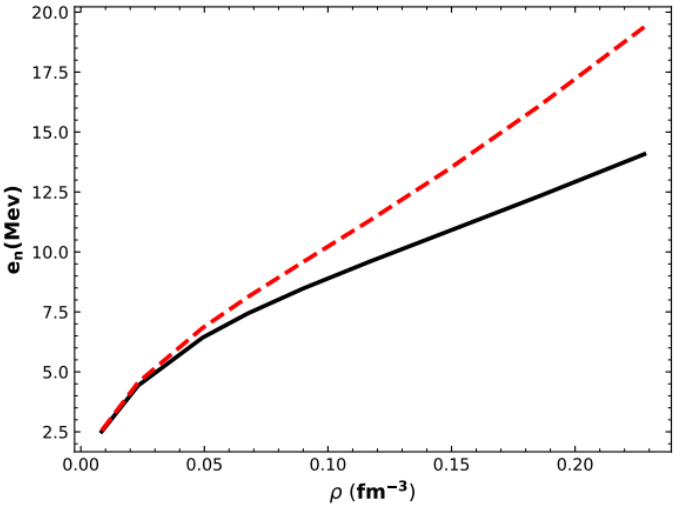

Figure 2. Energy per neutron in NM as a function of NM density. Solid black: original N^{3}LO(450) potential; Red dash: modified version. See text for details.

above 100 MeV. We then calculate the EoS of NM with the modified potential, see Figure 2. Around saturation, the energy moves up by about 25%, while the (very sensitive) slope and closely related pressure increase by a factor of 1.75. This comparison is shown in Table 1. In other words, the "modified" phase shifts are not disastrous, but the slope of the NM EoS changes dramatically.

Notice that our modified interaction is only very little different from the original interaction below 100 MeV, confirming extreme sensitivity of the neutron matter slope (and thus the slope of the symmetry energy) to the description of the isovector component of the NN interaction. On the other hand, this simple exercise suffices to demonstrate that relaxing or abandoning the constraint of free-space NN data can produce dramatic changes in L (and thus the neutron skin).

Table 1. The energy per neutron, its slope, and the pressure at a density of 0.155 fm^{-3} with the original N^{3}LO(450) potential and the modified version as explained in the text. Only the 2NF is included.

Calculated quantity		N^{3}LO(450)	modified potential
$e_n(\rho_0)$	(MeV)	11.11	13.88
$\left(\frac{\partial e_n(\rho)}{\partial \rho}\right)_{\rho_0}$	(MeV/fm^{-3})	39.79	70.03
$P(\rho_0)$	(MeV/fm^3)	0.956	1.68

The freedom to modify a model in such a way that isovector properties (such as the slope of the NM EoS) vary while retaining good fits to nuclei and nuclear matter, is the mechanism that generates the popular correlations from mean-field models. However, free-space NN data do not enter in this picture, contrary to the basic principle of *ab initio* predictions. Also, variations within the model parameter space are generally applied to predefined analytical expressions, such as power laws of the density.

4 Symmetry Energy and Neutron Skin: Predictions and Measurements

In Table 2, we show our latest results for the symmetry energy and closely related quantities, all of which are on the smaller side of the current range of predictions and measurements. We note that these values are typical of *ab initio* predictions based on chiral EFT, as well as a number of nuclear experiments [5] and far from the findings of PREX-II [6].

Table 2. Our predictions for: the symmetry energy at saturation, the L parameter, the neutron skin of ^{208}Pb, and the radius of a neutron star with mass equal to 1.4 solar masses [2,3].

Calculated quantity		N^{3}LO(450) prediction
$e_{\rm sym}(\rho_0)$	(MeV)	31.3 ± 0.8
L	(MeV)	50 ± 8.0
S(^{208}Pb)	(fm)	1.3 – 1.7
$R_{1.4}$	(km)	11.96 ± 0.80

The parity-violating experiment with ^{48}Ca has been recently completed [7]. The extracted neutron skin is $S = (0.121 \pm 0.026 \pm 0.024)$ fm. This small value would not be expected based on the PREX-II results, as the two nuclei are not very different in terms of isospin asymmetry, see Figure 3, where the neutron skin of selected nuclei is shown *vs.* the isospin asymmetry, $(N-Z)/A$. The predictions are from Ref. [8].

Table 3. Summary of recent ab initio predictions for the neutron skin in ^{208}Pb and in ^{48}Ca.

Nucleus	Neutron skin (fm)–Source	
^{208}Pb	0.14–0.20	Ref. [4]
^{48}Ca	0.120–0.150	Ref. [10]
^{208}Pb	0.184–0.236	Ref. [11]
^{48}Ca	0.114–0.186	Ref. [11]

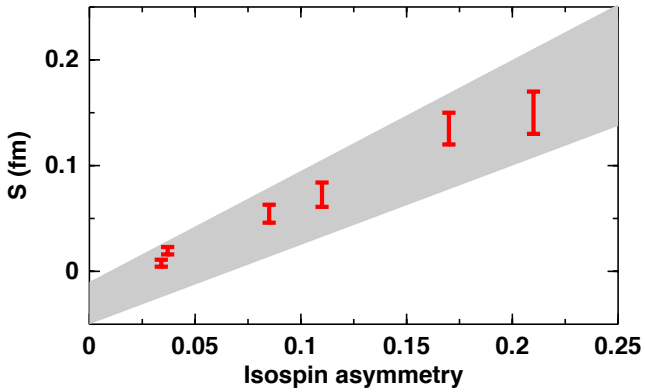

Figure 3. Red bars: Neutron skin of ^{58}Ni, ^{27}Al, ^{59}Co, ^{90}Zr, ^{48}Ca, and ^{208}Pb [8]. The shaded area is bounded by linear fits to the data [9].

In Table 3, we display some recent *ab initio* predictions for the neutron skin in ^{48}Ca and ^{208}Pb. Note, though, that the value for ^{208}Pb in Ref. [11] was obtained from a linear regression fitted to lighter nuclei.

The points in Figure 4 are extracted from Ref. [12] and give the neutron skin in ^{48}Ca (left) and ^{208}Pb (right) obtained from a variety of experimental methods.

In summary, CREX and PREX-II outcomes are not consistent with each other. We anxiously await to hear from MREX (Mainz Radius Experiment) at

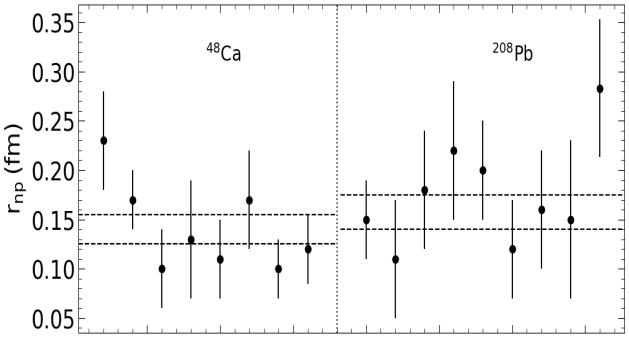

Figure 4. The neutron skin in ^{48}Ca (left) and ^{208}Pb (right) extracted from various experiments including elastic proton scattering, elastic polarized proton scattering, pionic atoms, pion scattering, α scattering, antiproton annihilation, coherent $\pi^0\gamma$ production. The sources for each of the points are given in Ref. [12]. The rightmost point for Calcium is the result from CREX, and the rightmost point for Lead is the result from PREX-II.

the MESA accelerator. The Mainz Radius EXperiment (MREX) will determine the neutron-skin thickness of ^{208}Pb with ultimate precision [13].

5 Low-Density Neutron Matter

A unitary Fermi gas is an idealized system of fermions with a zero-range interaction having an infinite (negative) scattering length. All properties of this interacting gas are simply proportional to the corresponding ones in the non-interacting system at the same density. The model of a dilute quantum gas can describe diverse systems and can be applied in different areas of physics. At the low temperatures required to observe quantum phenomena in a dilute gas, the type of fermions and the exact form of the interaction become unimportant for the macroscopic properties of the system. For these reasons, results from the field of cold gases can give insight into systems such as NM at subnuclear densities. This unique feature of interacting Fermi gases – unitarity – can be generalized to any system of fermions subjected to mutual interactions with diverging scattering lengths. The unitary limit was first introduced in 1999 by Bertsch [14], who proposed to model low-density neutron matter as a Fermi gas where

$$r_e \ll k_F^{-1} \ll |a_s| \,, \quad \text{implying} \quad k_F |a_s| \gg 1 \,. \tag{5}$$

Universality of unitary systems implies that the ground state energy at the unitary limit should be given by

$$E(k_F) = \xi E_{\rm FG}(k_F) \,, \tag{6}$$

where ξ is known as the Bertsch parameter and $E_{FG}(k_F)$ is the energy of the corresponding non-interacting Fermi gas. Measurements of the Berstch parameter with ultra-cold atomic gases reported values ranging from ~ 0.36 to ~ 0.51.

A few years ago, Tews *et al.* [15] proposed the existence of a lower limit on the energy of NM based on unitarity. With an eye on recent results from electroweak scattering, here we revisit that discussion for the purpose of emphasising the importance of low-energy constraints for NM and the symmetry energy [16].

A lower limit on the energy of NM based on unitarity implies:

$$E_{\rm NM}(\rho) \geq E_{\rm UG}(\rho) \,, \tag{7}$$

where UG stands for unitary gas. Thus:

$$E_{\rm NM}(\rho) \geq E_{\rm UG}(\rho) = \xi_0 E_{\rm FG}(\rho) \,, \tag{8}$$

where ξ_0 is the Bertsch parameter, and $E_{\rm FG}$ is the energy of the non-interacting Fermi gas,

$$E_{\rm FG} = \frac{3\hbar^2 k_F^2}{10m} \,, \qquad k_F = (3\pi^2\rho)^{1/3} \,. \tag{9}$$

Thus, in the parabolic approximation to the symmetry energy, Eq. (2), we can write

$$E_{\rm sym}(\rho) = E_{\rm NM}(\rho) - E_{\rm SNM}(\rho) \geq E_{\rm UG}(\rho) - E_{\rm SNM}(\rho)\,, \tag{10}$$

where SNM signifies symmetric nuclear matter.

There exist "established" expansions of the energy in SNM in terms of the saturation parameters $E_0 = E(\rho_0)$ and the incompressibility K_0. The next term in the expansion is the skewness, Q_0, which is poorly known. To streamline the notation, we express density in units of saturation density and define $u = \rho/\rho_0$. The expansion of the SNM energy is then written as

$$E_{\rm SNM}(u) = E_{\rm SNM}(u=1) + \frac{K_0}{18}(u-1)^2 + \frac{Q_0}{162}(u-1)^3 + \cdots\,, \tag{11}$$

where $u = 1$ at $\rho = \rho_0 = 0.16$ fm^{-3}, $E_{\rm SNM}(u=1) = E_0 = -16$ MeV, and $K_0 = 230$ MeV. In Ref. [15], some estimates are made for Q_0. Clearly, reliable constraints on these parameters must be available from independent sources. It must be emphasized, though, that the specific values are not very relevant for the present discussion, which is a qualitative demonstration of how the unitarity constraint propagates.

From Eq. (10) and Eq. (11), ignoring higher-order terms in the SNM expansion, one can write

$$E_{\rm sym}(u) \geq E_{\rm UG}(u) - \Big(E_0 + \frac{K_0}{18}(u-1)^2 + \frac{Q_0}{162}(u-1)^3\Big)\,. \tag{12}$$

Furthermore, replacing the symmetry energy with its well-know expansion about saturation density,

$$\begin{aligned} E_{\rm sym}(u) &= E_{\rm sym,0} + \frac{L}{3}(u-1) + \frac{K_{\rm sym}}{18}(u-1)^2 + \cdots \ldots\,, \\ E_{\rm sym,0} &= E_{\rm sym}(u=1)\,, \end{aligned} \tag{13}$$

one can turn Eq. (12) into a constraint for L, the slope of the symmetry energy at saturation. For the purpose of this exercise [15], and for consistency, one term beyond the leading order is retained in both the expansion of the symmetry energy and the SNM energy, that is, $Q_0 = K_{\rm sym} = 0$. Thus,

$$E_{\rm sym}(u) \approx E_{\rm sym,0} + \frac{L}{3}(u-1)\,, \tag{14}$$

and Eq. (12) is written as

$$E_{\rm sym,0} + \frac{L}{3}(u-1) \geq E_{UG}(u) - \Big(E_0 - \frac{K_0}{18}(u-1)^2\Big)\,. \tag{15}$$

So, for a chosen value of $E_{\rm sym,0}$, one can write, for $u > 1$:

$$L \geq \frac{3}{(u-1)}\Big(E_{\rm UG}(u) - E_0 - \frac{K_0}{18}(u-1)^2 - E_{\rm sym,0}\Big)\,, \tag{16}$$

and, for $u < 1$:

$$L \leq \frac{3}{(u-1)}\left(E_{\rm UG}(u) - E_0 + \frac{K_0}{18}(u-1)^2 - E_{\rm sym,0}\right), \tag{17}$$

thus setting a lower and an upper limit to L. Proceeding along these lines, one can then construct a contour in the $(L - E_{\rm sym,0})$ plane. Obviously, unitarity is one of many constraints, from both microscopic theory and experiments, to be considered carefully and vetted for consistency. The focal point of this discussion is to emphasize the inherent connection between NM and low-energy few-nucleon systems, due to the proximity of few-nucleon systems to the unitary limit.

6 Conclusion

Neutron matter from low to high density offers the opportunity to test nuclear forces in nuclear as well as astrophysical systems.

The density dependence of the symmetry energy, which controls the pressure in NM, continues to be debated. From the current status of microscopic predictions and experiments, we conclude that the large ^{208}Pb neutron skin extracted from PREX-II is the outlier. The upcoming MREX experiment should be quite insightful.

Within our overarching theme to advance microscopic nuclear physics, we have embarked in the challenging task of computing the chiral 3NF at N^{4}LO. Convergence at N^{3}LO needs to be on robust grounds. The 3NF at N^{4}LO will generate non-locality, and, perhaps, the additional softness needed to solve one or more outstanding problems in nuclear structure [17].

Acknowledgements

I am deeply grateful to the Organizers for the opportunity to participate in this workshop series and for the warm hospitality.
This work was supported by the U.S. Department of Energy under Award No. DE-FG02-03ER41270.

References

[1] S. Weinberg, *Phys. Lett. B* **295** (1992) 114.
[2] F. Sammarruca, R. Millerson, *Phys. Rev. C* **104** (2021) 034308.
[3] F. Sammarruca, R. Millerson, *Phys. Rev. C* **104** (2021) 064312.
[4] B. Hu, W. Jiang, T. Miyagi, Z. Sun, A. Ekstrm, C. Forssen, G. Hagen, J. D. Holt, T. Papenbrock, S. Ragnar Stroberg, I. Vernon, *Nat. Phys.* **18** (2021) 1196.
[5] Y. Lin, J. Holt, *EPJ* **55** (2019) 209.
[6] B.T. Reed, F.J. Fattoyev, C.J. Horowitz, J. Piekarewicz, *Phys. Rev. Lett.* **126** (2021) 172503.
[7] The CREX Collaboration, *Phys. Rev. Lett.* **129** (2022) 042501.
[8] F. Sammarruca, *Phys. Rev. C* **105** (2022) 064303.

[9] W.J. Swiatecki, A. Trzcinska, J. Jastrzebski, *Phys. Rev. C* **71** (2005) 047301.
[10] G. Hagen *et al.*, *Nat. Phys.* **12** (2016) 186.
[11] S.J. Novario *et al.*, *Phys. Rev. Lett.* **130** (2023) 032501.
[12] J.M. Lattimer, *Particles* **6** (2023) 30.
[13] D. Becker *et al.*, arXiv:1802.04759 [nucl-ex].
[14] G.F. Bertsch, *Int. J. Mod. Phys. B* **15** (2001) 10.
[15] I. Tews, J.M. Lattimer, A. Ohnishi, E.E. Kolomeitsev, arXiv:1611.07133 [nucl-th].
[16] Francesca Sammarruca, in press, *Physical Review C*.
[17] R. Machleidt, arXiv:2307.06416.